Proc. Natl. Acad. Sci. USA
Vol. 91, pp. 5315–5319, June 1994
Biochemistry

Fast photoinduced electron transfer through DNA intercalation

(luminescence quenching/long-range electron transfer/metallointercalators/DNA mediation/spectroscopic probes)

CATHERINE J. MURPHY†, MICHELLE R. ARKIN†, NARESH D. GHATLIA‡, STEFAN BOSSMANN‡, NICHOLAS J. TURRO‡§, AND JACQUELINE K. BARTON†§

†Division of Chemistry and Chemical Engineering, Beckman Institute, California Institute of Technology, Pasadena, CA 91125; and ‡Department of Chemistry, Columbia University, New York, NY 10027

Contributed by Nicholas J. Turro, January 18, 1994

ABSTRACT **We report evidence for fast photoinduced electron transfer mediated by the DNA helix that requires metal complexes that are avid intercalators of DNA. Here the donor bis(phenanthroline)(dipyridophenazine)ruthenium(II) [Ru(phen)$_2$dppz^{2+}] and acceptor bis(9,10-phenanthrenequinone diimine)(phenanthroline)rhodium(III) [Rh(phi)$_2$phen^{3+}] intercalate into DNA with $K_b > 10^6$ M^{-1}. Luminescence quenching experiments in the presence of two different lengths of DNA yield upward-curving Stern–Volmer plots and the loss of luminescence intensity far exceeds the change in emission lifetimes. In the presence of a nonintercalative electron acceptor, Ru(NH$_3$)$_6^{3+}$, Ru(phen)$_2$dppz^{2+} luminescence is quenched much less efficiently compared to that found for the intercalative Rh(phi)$_2$phen^{3+} quencher and follows linear Stern–Volmer kinetics; steady-state and time-resolved Stern–Volmer plots are comparable in scale. These experiments are consistent with a model involving fast long-range electron transfer between intercalators through the DNA helix.**

Understanding electron transfer over long distances is essential to the characterization of fundamental redox processes such as oxidative phosphorylation and is surely critical to the design of artificial photosynthetic systems and electroactive sensors (1, 2). Experiments in many laboratories have focused on measurements of electron transfer rates between metal centers over long distances in proteins or protein pairs as a function of distance, driving force, and the intervening medium (3, 4). Although the notion of charge transfer in nucleic acids has been postulated for some time (5–7), only recently has DNA been examined as a medium for electron transfer reactions (8–11). Experiments with radiation-damaged DNA have suggested the importance of DNA-mediated electron transfer with regard to nucleic acid-based disease. Studies of DNA under extreme conditions (77 K, neutron bombardment) have suggested that radical species can migrate up to 100 bp away from the initial lesion (12, 13). Pulse radiolysis experiments of the cytotoxin daunorubicin intercalated into DNA reveal that this electronic migration is comparable in rate to excess electron mobility in conducting polymers (14). This dissipation of charge may actually be a mechanism by which redox damage to DNA at localized sites may be avoided.

We have previously found that the rate of electron transfer between transition metal complexes is enhanced in the presence of DNA. Cationic tris(phenanthroline)metal complexes were used as donor–acceptor pairs (8, 10) since these complexes had been shown to bind to DNA noncovalently ($K_b \approx 5 \times 10^3$ M^{-1}) through primarily two modes: (*i*) intercalation and (*ii*) surface binding (15–18). In these experiments, the donor was photoexcited Ru(L)$_3^{2+}$, while the acceptors were M(L)$_3^{3+}$, M = Rh(III), Co(III), or Cr(III) and L = 1,10-phenanthroline or 2,2′-bipyridine. How DNA might mediate these electron transfer processes was difficult to discern in part because of the rapid equilibration between binding modes and positions of donors and acceptors (10, 19).

Here we report evidence for fast DNA-mediated electron transfer between metal complexes that are avid intercalators of DNA. In this system, both donor and acceptor intercalate into DNA with $K_b > 10^6$ M^{-1}. The donor, photoexcited bis(phenanthroline)(dipyridophenazine)ruthenium(II) [Ru(phen)$_2$dppz^{2+}] (Fig. 1), shows no luminescence in aqueous solution but, in the presence of DNA, where the phenazine nitrogens are protected from water through intercalation of the dppz ligand, intense luminescence is observed (20, 21). This luminescence is sensitive to the DNA base composition and conformation in the helical stack (22). Spectroscopic and DNA unwinding assays on Ru(phen)$_2$dppz^{2+} and its derivatives have provided strong support for intercalation by the dppz ligand (20, 22–25). The acceptor is bis(9,10-phenanthrenequinone diimine)(phenanthroline)rhodium(III) [Rh(phi)$_2$phen^{3+}] (Fig. 1). Rhodium(III) complexes containing phi bind tightly to nucleic acids via intercalation (26, 27). Two-dimensional NMR experiments have provided direct evidence for intercalation of phi complexes in the DNA major groove through the phi ligand (ref. 28; J. G. Collins, T. P. Shields, and J.K.B., unpublished data). Phi complexes of rhodium cleave DNA and RNA upon photoactivation and thus are also useful as probes of higher-order structures in nucleic acids and as high-resolution DNA photofootprinting reagents (29–35). The absorption spectrum of Ru(phen)$_2$dppz^{2+} is characterized by a metal-to-ligand charge transfer transition centered on the dppz ligand, and the emission from this state in nonaqueous solution can be quenched by electron acceptors (36). The lowest energy absorption band of Rh(phi)$_2$phen^{3+} is centered on the phi ligand (37). Thus, photoinduced electron transfer may be directed in the presence of DNA from the ruthenium(II) donor to the rhodium(III) acceptor and be mediated by the stacked bases (Fig. 1).

Experiments have also been recently conducted in our laboratory on derivatives of these intercalating donors and acceptors covalently attached to the 5′ termini of complementary oligonucleotides (38). The experiments described here, using noncovalently bound species, permit a comparison of donors and acceptors that bind DNA through either intercalative or nonintercalative binding modes and thus the ability to explore the binding requirements for fast photoinduced electron transfer.

MATERIALS AND METHODS

Chemicals. [Ru(phen)$_2$dppz]Cl$_2$ and [Rh(phi)$_2$phen]Cl$_3$ were prepared as described in the literature (21, 29).

The publication costs of this article were defrayed in part by page charge payment. This article must therefore be hereby marked "*advertisement*" in accordance with 18 U.S.C. §1734 solely to indicate this fact.

Abbreviations: Ru(phen)$_2$dppz^{2+}, bis(phenanthroline)(dipyridophenazine)ruthenium(II); Rh(phi)$_2$phen^{3+}, bis(9,10-phenanthrenequinone diimine)(phenanthroline)rhodium(III).

§To whom reprint requests should be addressed.

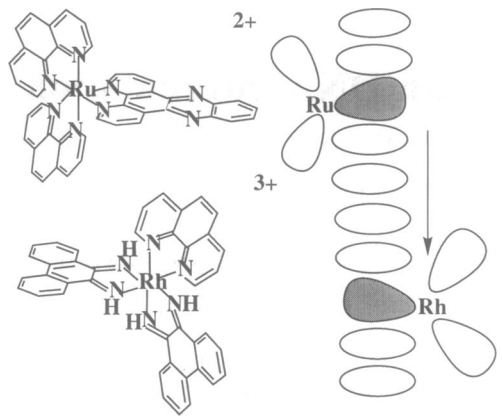

FIG. 1. Structures of donor and acceptor complexes $Ru(phen)_2dppz^{2+}$ and $Rh(phi)_2phen^{3+}$ and a schematic illustrating a possible electronic pathway from the $Ru(phen)_2dppz^{2+}$ donor (metal-to-ligand charge transfer to the intercalated dppz ligand; shaded ellipse) through the stacked bases of DNA to the $Rh(phi)_2phen^{3+}$ acceptor (intercalated phi ligand; shaded ellipse).

$[Ru(NH_3)_6]Cl_3$ was a gift of I.-J. Chang (California Institute of Technology). Metal complex concentrations were determined spectrophotometrically: $2.1 \times 10^4\ M^{-1}\cdot cm^{-1}$ at 440 nm for $[Ru(phen)_2dppz]Cl_2$, $2.2 \times 10^4\ M^{-1}\cdot cm^{-1}$ at 360 nm for $[Rh(phi)_2phen]Cl_3$, and $460\ M^{-1}\cdot cm^{-1}$ at 276 nm for $[Ru(NH_3)_6]Cl_3$. Calf thymus DNA (Pharmacia) was dialyzed against buffer before use. The oligonucleotide 5′-d(CGCGATATGGGCGCATTAACCAGAATTC)-3′ and its complement were synthesized on an Applied Biosystems model 394 DNA/RNA synthesizer using standard phosphoramidite chemistry (39) and purified by HPLC (C_{18} column; eluant, triethylamine/acetic acid/acetonitrile). Tris buffer (5 mM Tris·HCl/50 mM NaCl, pH 7.2) made up with Millipore filtered water was used for all aqueous experiments.

Photophysical Measurements. Ultraviolet-visible absorption spectra were taken on a Hewlett–Packard model 8452 diode array spectrophotometer. Steady-state luminescence measurements were performed on an SLM Instruments (Urbana, IL) model 8000 spectrofluorimeter with excitation at either 440 or 480 nm. Alternatively, intensity data were calculated from the integration of the decay traces in the time-resolved experiment. The time-resolved laser system has been described (21). Decays were the average of at least 500 shots. Traces were fit to a multiexponential program using least-squares minimization. Excitation energies ranged from 0.8 to 1.0 mJ; time resolution was ≈10 ns. All measurements were taken at ambient temperature in air.

Cyclic Voltammetry. Cyclic voltammetry was performed on $[Ru(phen)_2dppz](PF_6)_2$ and $[Rh(phi)_2phen](PF_6)_3$ in *N,N*-dimethylformamide with 100 mM tetrabutylammonium hexafluorophosphate as the supporting electrolyte. $[Ru(NH_3)_6]Cl_3$ was dissolved in water with 1 M NaCl as the supporting electrolyte. Data were collected on a BAS (West Lafayette, IN) CV-25 voltammograph with a glassy carbon working electrode and a 3 M Ag/AgCl reference electrode and were recorded at 100 mV/s on a BAS X-Y chart recorder. Values are reported relative to the standard hydrogen electrode by adding 0.22 V to experimentally determined reduction potentials.

Photocleavage of Radiolabeled Oligonucleotides. Oligonucleotides (28-mer) were 5′-^{32}P-end-labeled using T4 polynucleotide kinase (Boehringer Mannheim) and [γ-^{32}P]ATP (NEN/DuPont); 500 μM (nucleotide) radiolabeled DNA was incubated with $Rh(phi)_2phen^{3+}$ (50 μM) in the presence and absence of $Ru(phen)_2dppz^{2+}$. Irradiations were performed at 313 nm [Oriel (Stamford, CT) Hg/Xe lamp] for 7 min and quantitation was accomplished by densitometry (LKB Ultroscan XL) of an autoradiogram of a 20% denaturing polyacrylamide gel.

RESULTS

Cyclic Voltammetry. Cyclic voltammetry was used to determine the redox potentials of metal complexes used in these studies. $Ru(phen)_2dppz^{2+}$ was found to be reversibly oxidized, with a potential of 1.63 V. The reduction of $Rh(phi)_2phen^{3+}$ was quasi-reversible with a potential of +0.02 V. For $Ru(NH_3)_6^{3+}$, in comparison, we find a reduction potential of +0.04 V in water. Errors for these measurements were estimated to be ±0.02 V. Driving forces for photoinduced electron transfer reactions were calculated by the equation

$$E^0(*D/D^+) = E^0(D/D^+) + E_{00}(*D),$$

where E_{00} of the photoexcited donor is 2.4 V (550 nm) and the ground state potential (E^0) is −1.63 V. Thus, the driving forces for photoinduced electron transfer are −0.79 V for $*Ru(phen)_2dppz^{2+}/Rh(phi)_2phen^{3+}$ and −0.81 V for $*Ru(phen)_2dppz^{2+}/Ru(NH_3)_6^{3+}$.

Quenching of $Ru(phen)_2dppz^{2+}$ by $Rh(phi)_2phen^{3+}$. Emission titrations of 10 μM $Ru(phen)_2dppz^{2+}$/1000 μM nucleotide calf thymus DNA with 0–100 μM $Rh(phi)_2phen^{3+}$ show that the overall intensity of luminescence drops by a factor of 3 up to ≈50 μM $Rh(phi)_2phen^{3+}$, and by 88% with 100 μM $Rh(phi)_2phen^{3+}$. The time-resolved luminescence of $Ru(phen)_2dppz^{2+}$ in the presence of DNA is characterized by a biexponential decay (20). From inspection of Fig. 2, it is clear that in the time-resolved experiment the Stern–Volmer parameters for each component are smaller at any given concentration of quencher than that found for the steady-state quenching by $Rh(phi)_2phen^{3+}$. For example, at 100 μM $Rh(phi)_2phen^{3+}$, the steady-state quenching (I_0/I) is ≈8.5, whereas at the same concentration, the time-resolved Stern–Volmer quenching (τ_0/τ) is ≈1.5. Inner filter effects were found to be negligible.

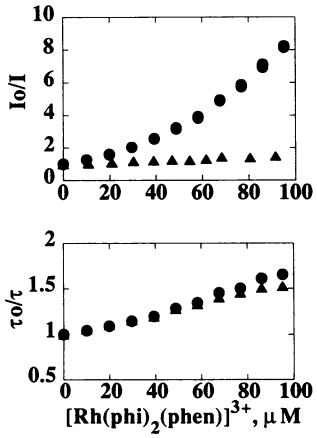

FIG. 2. Stern–Volmer plots of $Ru(phen)_2dppz^{2+}$ luminescence quenching by $Rh(phi)_2phen^{3+}$, measured by integrated intensity (*Upper*) and by luminescence lifetime decay (*Lower*) in the presence of calf thymus DNA and in ethanol. Reaction conditions in DNA were 10 μM $Ru(phen)_2dppz^{2+}$, 1000 μM nucleotide DNA, 0–100 μM $Rh(phi)_2phen^{3+}$ in buffer (5 mM Tris·HCl/50 mM NaCl, pH 7.2) at ambient temperature. (*Upper*) Integrated intensity of $Ru(phen)_2dppz^{2+}$ emission as a function of $Rh(phi)_2phen^{3+}$ concentration in the presence of calf thymus DNA (●) and in ethanol (▲). (*Lower*) Long lifetime component (●) and short lifetime component (▲) of $Ru(phen)_2dppz^{2+}$ emission as a function of $Rh(phi)_2phen^{3+}$ concentration in the presence of calf thymus DNA. Measurements were made in triplicate.

The quenching of $Ru(phen)_2dppz^{2+}$ luminescence by $Rh(phi)_2phen^{3+}$ in the absence of DNA cannot be performed in aqueous solution since the ruthenium complex does not luminesce (20). $Ru(phen)_2dppz^{2+}$ does emit in ethanol, however, and its luminescence decays as a single exponential with a lifetime of ≈160 ns. Titration of a 10 μM solution with 0–100 μM $Rh(phi)_2phen^{3+}$ yields little change in emission intensity (Fig. 2). $Ru(phen)_3^{2+}$, unlike $Ru(phen)_2dppz^{2+}$, does luminesce in aqueous buffered solution in the absence of DNA, and therefore the quenching of $Ru(phen)_3^{2+}$ luminescence by $Rh(phi)_2phen^{3+}$ in buffer provides an appropriate control with similar driving force. The results (data not shown) parallel those found for the luminescence quenching of $Ru(phen)_2dppz^{2+}$ by $Rh(phi)_2phen^{3+}$ in ethanol.

Luminescence quenching was also examined on an oligonucleotide duplex 28 bp long. The luminescence decay characteristics of $Ru(phen)_2dppz^{2+}$ bound to the 28-mer are comparable to that of $Ru(phen)_2dppz^{2+}$ bound to calf thymus DNA. Bound to calf thymus DNA, the excited-state lifetimes of $Ru(phen)_2dppz^{2+}$ are 725 ns (20%) and 125 ns (80%), while bound to the 28-mer the excited ruthenium complex also decays as a biexponential with lifetimes of 790 ns (25%) and 130 ns (75%); lifetime measurements have an uncertainty of 10%. A dramatic loss in the integrated emission intensity of $Ru(phen)_2dppz^{2+}$ bound to the 28-mer is observed (Fig. 3). The scale of the intensity losses exceeds that found for long calf thymus DNA at identical metal/nucleotide ratios [up to a factor of 33 at 100 μM $Rh(phi)_2phen^{3+}$]. However, as was found in the case of long DNA, the variation in excited-state decay kinetics with increasing $Rh(phi)_2phen^{3+}$ concentration is modest compared to the steady-state changes.

Time-resolved luminescence decay experiments of the $Ru(phen)_2dppz^{2+}$/calf thymus DNA/$Rh(phi)_2phen^{3+}$ system showed no residual decay of the ruthenium lumophore within the 10-ns resolution of a nanosecond instrument. Preliminary studies by picosecond transient absorption indicate quenching rates on the order of 120 ps (A. Hoermann, E. Olson, E. Stemp, M.R.A., P. Barbara, and J.K.B., unpublished data).

Quenching with Nonintercalating Complexes in the Presence of DNA. We also examined the effect of a known, nonintercalating electron transfer quencher of Ru(II) polypyridyl emission, $Ru(NH_3)_6^{3+}$ (40, 41), on the luminescence of intercalated $Ru(phen)_2dppz^{2+}$. The measured driving force for electron transfer to $Ru(NH_3)_6^{3+}$ is slightly greater than that found for $Rh(phi)_2phen^{3+}$. Quenching of the luminescence of 10 μM $Ru(phen)_2dppz^{2+}$/1000 μM nucleotide calf thymus DNA with 0–100 μM $Ru(NH_3)_6^{3+}$ yields a linear Stern–Volmer plot (Fig. 4). Importantly, quenching of each of the time-resolved components for this system also yields linear Stern–Volmer plots. Moreover, Stern–Volmer parameters for each component are roughly the same at any given concentration of quencher as that found for the steady-state

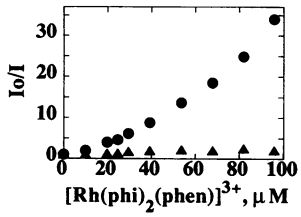

FIG. 3. Stern–Volmer plots of $Ru(phen)_2dppz^{2+}$ luminescence quenching by $Rh(phi)_2phen^{3+}$, measured by integrated intensity (●) and by luminescence lifetime decay (▲) in the presence of a 28-bp duplex oligonucleotide. Quenching of both lifetime components is indistinguishable on this scale. Reaction conditions were 10 μM $Ru(phen)_2dppz^{2+}$, 1000 μM nucleotide DNA, 0–100 μM $Rh(phi)_2phen^{3+}$ in buffer (5 mM Tris·HCl/50 mM NaCl, pH 7.2) at ambient temperature.

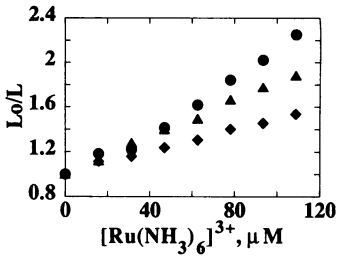

FIG. 4. Stern–Volmer plots of $Ru(phen)_2dppz^{2+}$ luminescence quenching by $Ru(NH_3)_6^{3+}$, measured by integrated intensity (●) and by luminescence lifetime decay in the presence of calf thymus DNA. Quenching of the longer-lived component (◆) and of the shorter-lived component (▲) is indicated. Reaction conditions were 10 μM $Ru(phen)_2dppz^{2+}$, 1000 μM nucleotide DNA, 0–100 μM $Ru(NH_3)_6^{3+}$ in buffer (5 mM Tris·HCl/50 mM NaCl, pH 7.2) at ambient temperature. Note that in contrast to the fully intercalative case, the quenching is dynamic and yields a linear Stern–Volmer plot.

quenching by $Rh(phi)_2phen^{3+}$; for example, at 100 μM $Rh(phi)_2phen^{3+}$, the steady-state quenching (I_0/I) is ≈2.0, whereas at the same concentration, the time-resolved Stern–Volmer quenching (τ_0/τ) is ≈1.8 for the short component and 1.5 for the long component. This behavior is significantly different from that observed with the intercalated $Rh(phi)_2phen^{3+}$ quencher and is clearly illustrated in Fig. 5, which shows the raw data from both titration experiments. Quenching of the DNA-bound ruthenium luminescence by $Ru(NH_3)_6^{3+}$ yields changes only in the excited-state lifetime of $Ru(phen)_2dppz^{2+}$, whereas quenching by $Rh(phi)_2phen^{3+}$ on the nanosecond time scale produces a decrease in both the lifetime and initial luminescent intensity. In a companion experiment, the luminescence of a nonintercalating electron donor, $Ru(2,2'\text{-bipyridine})_3^{2+}$, was unchanged by the addition of $Rh(phi)_2phen^{3+}$ in the presence of DNA (data not shown).

Photocleavage Assay. The fact that phi complexes of rhodium promote DNA strand cleavage with photoactivation can be used advantageously in exploring the distribution of donors and acceptors on the DNA helix. Since cleavage by the rhodium complex is almost but not completely sequence

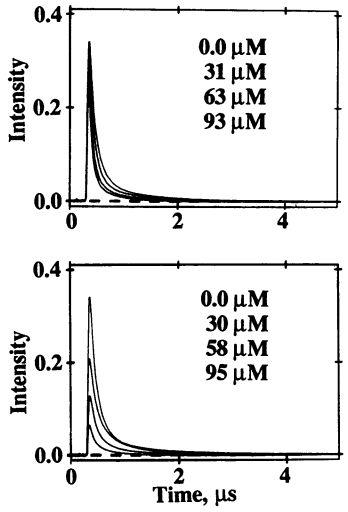

FIG. 5. (*Upper*) Luminescence decay traces of 10 μM $Ru(phen)_2dppz^{2+}$ in the presence of 1000 μM nucleotide calf thymus DNA as a function of increasing $Ru(NH_3)_6^{3+}$ concentration. (*Lower*) Luminescence decay traces of 10 μM $Ru(phen)_2dppz^{2+}$ in the presence of 1000 μM nucleotide calf thymus DNA as a function of increasing $Rh(phi)_2phen^{3+}$ concentration. Note that quenching by $Ru(NH_3)_6^{3+}$ produces changes in lifetime with a constant initial intensity, while quenching by the rhodium intercalator leads to striking decreases in the initial luminescence intensity.

neutral (29–35), we can examine whether cooperative or anticooperative binding of the ruthenium complex leads to a change in distribution of rhodium cleavage sites. Using densitometry, we find that the cleavage distribution is unchanged in the presence of ruthenium, consistent with the random distribution of both metal complexes on DNA.

DISCUSSION

Binding Modes of the Metal Complexes to DNA. The luminescence of DNA-bound $Ru(phen)_2dppz^{2+}$ is characterized by a biexponential decay in the time-resolved experiment, supporting the notion of dual binding modes for the complex (22, 23). The long-lived component of the emission, $\tau_1 \approx 725$ ns for calf thymus DNA in the absence of quencher, is assigned to an intercalated species in which the dppz ligand is directed perpendicular to the long axis of the base pair. The short-lived component of the emission, $\tau_2 \approx 120$ ns for calf thymus DNA in the absence of quencher, is assigned to a species in which the dppz ligand is intercalated in a "side-on" fashion, almost parallel to the long axis of the base pair, exposing one of the phenazine nitrogens to the aqueous solvent. This notion is consistent with the time-resolved quenching behavior observed for surface-bound $Ru(NH_3)_6^{3+}$, where the solvent-accessible, short component is quenched with roughly twice the efficiency of the long component (Fig. 4).

It should be noted that we and others have found enantioselective discrimination in the binding and spectroscopic characteristics of many ruthenium complexes bound to double-helical DNA (8, 16, 21, 24). Here experiments have been carried out with *rac*-$Ru(phen)_2dppz^{2+}$, where ≈80% of the luminescent intensity may be attributed to the Δ-isomer bound to DNA. The luminescence of both Λ- and Δ-$Ru(phen)_2dppz^{2+}$ in the presence of DNA decays as a biexponential, likely reflecting two intercalative binding modes for each enantiomer.

Earlier studies have shown that $Rh(phi)_2phen^{3+}$ binds by intercalation with a binding affinity comparable (slightly lower) to $Ru(phen)_2dppz^{2+}$ (27, 28, 37). While the complexes bind competitively, at the metal/DNA ratios used in these studies the rhodium complex does not displace the ruthenium complex; the binding site size for each is ≈4 bp.

Luminescence Quenching of DNA-Bound $Ru(phen)_2dppz^{2+}$ by $Rh(phi)_2phen^{3+}$ vs. $Ru(NH_3)_6^{3+}$. The steady-state and time-resolved Stern–Volmer parameters for the luminescence quenching of DNA-bound photoexcited $Ru(phen)_2dppz^{2+}$ by $Ru(NH_3)_6^{3+}$ are of comparable magnitude (Figs. 4 and 5). When the Stern–Volmer constants for steady-state and time-resolved measurements are identical, it can be assumed that the system is governed by "dynamic" quenching in which the luminescence intensity decrease occurs through a dynamic process, such as molecular diffusion, which is slow relative to the inherent luminescence decay in the absence of quencher (42, 43). Thus, the results of quenching of $Ru(phen)_2dppz^{2+}$ by $Ru(NH_3)_6^{3+}$ in the presence of calf thymus DNA are consistent with a mechanism involving at least one diffusing partner. Since luminescence polarization studies reveal that $Ru(phen)_2dppz^{2+}$ is essentially immobile on DNA during its excited state lifetime (21), $Ru(NH_3)_6^{3+}$ must be the diffusing species.

In contrast to the linear Stern–Volmer plots and the comparable Stern–Volmer constants observed in the $Ru(phen)_2dppz^{2+}$/calf thymus DNA/$Ru(NH_3)_6^{3+}$ experiments, the $Ru(phen)_2dppz^{2+}$/calf thymus DNA/$Rh(phi)_2phen^{3+}$ system shows nonlinear, upward-curving steady-state Stern–Volmer plots and much smaller Stern–Volmer parameters derived from time-resolved measurements than for the steady-state measurements (Fig. 2). Such a difference in Stern–Volmer parameters is consistent with the occurrence of at least two quenching mechanisms, one of which is complete on a time scale that is fast relative to the resolution in the time-resolved experiment and a second that is slow relative to this time scale (42–44). The latter is likely the result of diffusional quenching. The former, which is termed static quenching, is typically either the result of the formation of ground-state complexes, which when excited undergo quenching that does not involve diffusion, or the result of "sphere of action" quenching, which requires that quenchers within a certain sphere of the excited molecule will quench the excited state on a time scale that is short relative to the resolution of the measurement (42–44). The lack of new absorption bands in absorbance titration experiments suggests that ground-state complex formation is not the dominant static quenching mode. The photocleavage experiments also lend strong support for the absence of ground-state complex formation.

Comparison to $M(phen)_3^{n+}$. The data reported here for $Ru(phen)_2dppz^{2+}$ donor and $Rh(phi)_2phen^{3+}$ acceptor complexes that both bind tightly to DNA contrast strongly with earlier data reported for simple $M(phen)_3^{n+}$ complexes [donor M = Ru(II); acceptor M = Rh(III), Cr(III), Co(III)] that bind much more weakly to DNA (8, 10). Both the earlier data and the data reported here show that DNA enhances the quenching rates compared to solvent alone. However, the $M(phen)_3^{n+}$ complexes yielded linear Stern–Volmer plots in which the steady-state and time-resolved slopes were of similar magnitude. Also the quenching observed for the $M(phen)_3^{n+}$ complexes was less efficient in the presence of sonicated calf thymus DNA (length, ≈200 bp) than in the presence of long calf thymus DNA (length, ≈10,000 bp) (8). It appears from these observations that the binding modes of the complexes to DNA intimately affect the quenching observed between bound complexes. The tris(phenanthroline)-metal complexes, which bind through two modes, intercalation and surface binding, are more facile in diffusing along the helical polymer and, owing to their smaller ligand surface for intercalation compared to phi and dppz, are less tightly stacked between the base pairs, likely with poorer overlap to facilitate long-range electron transfer quenching through a DNA "π-way."

For $M(phen)_3^{n+}$ complexes, quenching is more efficient for long strands of calf thymus DNA than for shorter helices (8). Here, the higher quenching efficiency of $Ru(phen)_2dppz^{2+}$ by $Rh(phi)_2phen^{3+}$ in the presence of the 28-mer compared to the quenching efficiency in the presence of long calf thymus DNA is inconsistent with primarily a diffusional mechanism for quenching. This behavior is to be expected if both $Ru(phen)_2dppz^{2+}$ and $Rh(phi)_2phen^{3+}$ are immobile on the time scale of the $Ru(phen)_2dppz^{2+}$ excited state lifetime, so that the quenching mechanism cannot involve diffusion of either complex. Since both $Ru(phen)_2dppz^{2+}$ and $Rh(phi)_2phen^{3+}$ are strong intercalators of DNA, when bound to the 28-mer, the complexes are either in contact or within the sphere of action and diffusion is not necessary for quenching to occur.

Electron Transfer vs. Energy Transfer. Other workers have examined Ru(II) diimine complex luminescence quenching by Rh(III) diimine complexes and find that electron transfer from photoexcited Ru(II) to Rh(III) is a major pathway for nonradiative decay (45–47). The redox potentials of $Ru(phen)_2dppz^{2+}$ and $Rh(phi)_2phen^{3+}$ indicate that the driving force for photoinduced electron transfer is reasonably high, close to −0.8 V. In our case, the Ru(III) and Rh(II) intermediates may not be sufficiently long-lived to observe on a nanosecond time scale, however (46). Transient absorption spectroscopic studies on shorter time scales (10^{-14}–10^{-10} s) as well as in other microheterogeneous systems are necessary to characterize these intermediates. Förster energy transfer, an alternative quenching mechanism, would require that

there be good spectral overlap between donor and acceptor (43); in our system, the emission band of the photoexcited $Ru(phen)_2dppz^{2+}$ is energetically well below that of the ground-state $Rh(phi)_2phen^{3+}$ absorbance. Förster energy transfer is also ruled out because our system does not involve singlet-singlet pairs. Thus, we assign the primary quenching mechanism as one involving electron transfer.

It is important to note that we cannot exclude a superexchange energy transfer mechanism (43) as contributing to the overall quenching we observe. This superexchange mechanism would still require the intermediacy of the double helix and has been considered as a form of electron transfer or exchange. Furthermore, such triplet exchange would be expected to decay even more rapidly with distance through the helix than would quenching through a single electron transfer.

Implications. We have shown that electronic communication between our metal complexes bound to DNA most likely proceeds by an electron transfer mechanism and that this electron transfer is fastest ($>10^9$ sec^{-1}) when both donor and acceptor are intercalators and when the DNA length is short (on the order of 28 bp). Also, since the persistence length of DNA is 500 Å (≈150 bp) (48), the 28-mer is expected to be relatively rigid. It is therefore remarkable that at a ruthenium concentration of 10 μM and a rhodium concentration of 40 μM, in the presence of 500 μM DNA base pairs, >80% of the ruthenium(II) luminescence is quenched on the nanosecond time scale; at these concentrations, given a random distribution of metal complexes on the helix, the average distance between metal complexes is estimated to be ≥35 Å. These results are fully consistent with experiments recently conducted in our laboratory using ruthenium and rhodium derivatives covalently attached to the 5′ termini of complementary oligonucleotides (38). Based on these observations, we propose that long-range electron transfer could occur on a picosecond time scale between intercalated complexes within discrete domains of electronically coupled, stacked bases.

Our data suggest that fast, long-range electron transfer may occur between metallointercalators that bind avidly to DNA. Electronic coupling through the double helix, which facilitates intramolecular electron transfer, may be modulated by the dynamics of base stacking. Thus, transition metal complexes may be useful in probing DNA dynamics, and the DNA polyanion may provide a synthetically amenable medium to explore long-range electron transfer processes.

We are grateful to Dr. J. Winkler for expert technical assistance. In addition, we thank the National Institutes of Health (Grant GM49216 to J.K.B.), the National Science Foundation (N.J.T.), and the Air Force Office of Scientific Research (N.J.T.) for their financial support, as well as the National Science Foundation (C.J.M. and M.R.A.) and the Deutsche Forschungsgemeinschaft (S.B.).

1. Marcus, R. A. & Sutin, N. (1985) *Biochim. Biophys. Acta* **811**, 265–322.
2. Bowler, B. E., Raphael, A. L. & Gray, H. B. (1990) *Prog. Inorg. Chem.* **38**, 259–322.
3. McLendon, G. & Miller, J. R. (1985) *J. Am. Chem. Soc.* **107**, 7811–7817.
4. Wuttke, D. S., Bjerrum, M. J., Winkler, J. R. & Gray, H. B. (1992) *Science* **256**, 1007–1009.
5. Hoffmann, T. A. & Ladik, J. (1964) *Adv. Chem. Phys.* **7**, 84–158.
6. Dee, D. & Baur, M. E. (1974) *J. Chem. Phys.* **60**, 541–560.
7. Clementi, E. & Corongiu, G. (1982) *Int. J. Quantum Chem. Quantum Biol. Symp.* **9**, 213–221.
8. Barton, J. K., Kumar, C. V. & Turro, N. J. (1986) *J. Am. Chem. Soc.* **108**, 6391–6393.
9. Fromherz, P. & Rieger, B. (1986) *J. Am. Chem. Soc.* **108**, 5361–5362.
10. Purugganan, M. D., Kumar, C. V., Turro, N. J. & Barton, J. K. (1988) *Science* **241**, 1645–1649.
11. Brun, A. M. & Harriman, A. (1992) *J. Am. Chem. Soc.* **114**, 3656–3660.
12. Cullis, P. M., McClymont, J. D. & Symons, M. C. R. (1990) *J. Chem. Soc. Faraday Trans.* **86**, 591–592.
13. Miller, J. H. & Swenberg, C. E. (1990) *Can. J. Phys.* **68**, 962–966.
14. Houee-Levin, C., Gardes-Albert, M., Rouscilles, A., Ferradini, C. & Hickel, B. (1991) *Biochemistry* **30**, 8216–8222.
15. Barton, J. K., Goldberg, J. M., Kumar, C. V. & Turro, N. J. (1986) *J. Am. Chem. Soc.* **108**, 2081–2090.
16. Pyle, A. M., Rehmann, J. P., Meshoyrer, R., Kumar, C. V., Turro, N. J. & Barton, J. K. (1989) *J. Am. Chem. Soc.* **111**, 3051–3058.
17. Rehmann, J. P. & Barton, J. K. (1990) *Biochemistry* **29**, 1701–1709.
18. Rehmann, J. P. & Barton, J. K. (1990) *Biochemistry* **29**, 1710–1717.
19. Orellana, G., Kirsch-De Mesmaeker, A., Barton, J. K. & Turro, N. J. (1991) *Photochem. Photobiol.* **54**, 499–509.
20. Friedman, A. E., Chambron, J.-C., Sauvage, J.-P., Turro, N. J. & Barton, J. K. (1990) *J. Am. Chem. Soc.* **112**, 4960–4962.
21. Friedman, A. E., Kumar, C. V., Turro, N. J. & Barton, J. K. (1991) *Nucleic Acids Res.* **19**, 2595–2602.
22. Jenkins, Y., Friedman, A. E., Turro, N. J. & Barton, J. K. (1992) *Biochemistry* **31**, 10809–10816.
23. Hartshorn, R. M. & Barton, J. K. (1992) *J. Am. Chem. Soc.* **114**, 5919–5925.
24. Hiort, C., Lincoln, P. & Norden, B. (1993) *J. Am. Chem. Soc.* **115**, 3448–3454.
25. Gupta, N., Grover, N., Neyhart, G. A., Singh, P. & Thorp, H. H. (1993) *Inorg. Chem.* **32**, 310–316.
26. Pyle, A. M., Long, E. C. & Barton, J. K. (1989) *J. Am. Chem. Soc.* **111**, 4520–4522.
27. Sitlani, A., Long, E. C., Pyle, A. M. & Barton, J. K. (1992) *J. Am. Chem. Soc.* **114**, 2303–2312.
28. David, S. S. & Barton, J. K. (1993) *J. Am. Chem. Soc.* **115**, 2984–2985.
29. Uchida, K., Pyle, A. M., Morii, T. & Barton, J. K. (1989) *Nucleic Acids Res.* **17**, 10259–10279.
30. Chow, C. S. & Barton, J. K. (1990) *J. Am. Chem. Soc.* **112**, 2839–2841.
31. Pyle, A. M., Morii, T. & Barton, J. K. (1990) *J. Am. Chem. Soc.* **112**, 9432–9434.
32. Huber, P. W., Morii, T., Mei, H.-Y. & Barton, J. K. (1991) *Proc. Natl. Acad. Sci. USA* **88**, 10801–10805.
33. Chow, C. S. & Barton, J. K. (1992) *Methods Enzymol.* **212**, 219–241.
34. Chow, C. S., Behlen, L. S., Uhlenbeck, O. C. & Barton, J. K. (1992) *Biochemistry* **31**, 972–982.
35. Chow, C. S., Hartmann, K. M., Rawlings, S. L., Huber, P. W. & Barton, J. K. (1992) *Biochemistry* **31**, 3534–3542.
36. Amouyal, E., Homsi, A., Chambron, J.-C. & Sauvage, J.-P. (1990) *J. Chem. Soc. Dalton Trans.* 1841–1845.
37. Pyle, A. M., Chiang, M. Y. & Barton, J. K. (1990) *Inorg. Chem.* **29**, 4487–4495.
38. Murphy, C. J., Arkin, M. R., Jenkins, Y., Ghatlia, N. D., Bossmann, S. H., Turro, N. J. & Barton, J. K. (1993) *Science* **262**, 1025–1029.
39. Beaucage, S. L. & Caruthers, M. H. (1981) *Tetrahedron Lett.* **22**, 1859–1862.
40. Lin, C. T. & Sutin, N. (1976) *J. Phys. Chem.* **80**, 97–105.
41. Ho, P. S., Frederick, C. A., Saal, D., Wang, A. H.-J. & Rich, A. (1987) *J. Biomol. Struct. Dynam.* **4**, 521–534.
42. Wagner, P. J. (1971) in *Creation and Detection of the Excited State*, ed. Lamola, A. A. (Dekker, New York), pp. 173–212.
43. Turro, N. J. (1978) *Modern Molecular Photochemistry* (Benjamin–Cummings, Menlo Park, CA).
44. Laws, W. R. & Contino, P. B. (1992) *Methods Enzymol.* **210**, 448–463.
45. Creutz, C., Keller, A. D., Sutin, N. & Zipp, A. P. (1982) *J. Am. Chem. Soc.* **104**, 3618–3627.
46. Kalyanasundaram, K., Gratzel, M. & Naazeeruddin, Md. K. (1992) *J. Phys. Chem.* **96**, 5865–5872.
47. Nozaki, K., Ohno, T. & Haga, M. (1992) *J. Phys. Chem.* **96**, 10880–10888.
48. Wang, J. C. & Giaever, G. N. (1988) *Science* **240**, 300–304.